Inorganica Chimica Acta, 186 (1991) 187–198

Transition metal complexes with sulfur ligands LXIII*. π-Electron delocalization and partial ruthenium sulfur multiple bonding in ruthenium bis-1,2-benzenedithiolate complexes: X-ray structure analyses and redox chemistry of $[Ru('S_2')_2(PMe_3)_2]^n$ ($n=0, -1$; $'S_2'^{2-}$ = 1,2-benzenedithiolate(2–))

Dieter Sellmann, Michael Geck, Falk Knoch** and **Matthias Moll**

Institut für Anorganische Chemie der Universität Erlangen-Nürnberg, Egerlandstrasse 1, D-8520 Erlangen (F.R.G.)

(Received January 2, 1991; revised April 9, 1991)

Abstract

In order to investigate specific properties of metal sulfur centers, anionic and neutral $[Ru('S_2')_2(PMe_3)_2]^n$ (**1**: $n=-1$; **2**: $n=0$; $'S_2'^{2-}$ = 1,2-benzenedithiolate(2–)) were synthesized from $RuCl_3 \cdot xH_2O$, $Na_2'S_2'$ and PMe_3 in the absence (**1**) or presence (**2**) of O_2. X-ray structure determinations of $(NMe_4)[Ru('S_2')_2(PMe_3)_2] \cdot CH_3OH$ (**1a**) (triclinic, $P\bar{1}$, $a=882.6(3)$, $b=935.1(2)$, $c=1800.1(4)$ pm, $\alpha=92.27(1)$, $\beta=92.58(2)$, $\gamma=94.60(2)°$, $Z=2$, $R/R_w=0.045/0.039$) and of $[Ru('S_2')_2(PMe_3)_2]$ (**2**) (monoclinic, $P2_1/c$, $a=927.3(3)$, $b=1012.0(3)$, $c=1220.2(5)$ pm, $\beta=102.35(3)°$, $Z=2$, $R/R_w=0.031/0.027$) show that in both complexes the Ru atoms are centers of symmetry and pseudooctahedrally surrounded by four sulfur and two *trans* phosphorus donors. The unit cell of **1a** contains two independent anions, one of which is solvated by two methanol molecules via S···H–O bridges. Analysis of structural data indicates extended π-electron delocalization over planar $Ru('S_2')_2$ entities in **1** and **2**. For anionic **1** this delocalization extends even to the phosphorus donors. The structural results are supported by UV–Vis/near-IR and magnetic data. $[Ru('S_2')_2(PMe_3)_2]^-$ (**1**) is readily oxidized by protons to yield neutral **2**, while homologous $[Fe('S_2')_2(PMe_3)_2]^-$ upon protonation yields $[Fe('S_2')_2]_2^{2-}$. Cyclovoltammetry of $(NBu_4)[Ru('S_2')_2(PMe_3)_2]$ (**1b**) and **2** revealed two quasi-reversible one-electron steps at very negative potentials (−0.6 and −1.6 V versus NHE) due to $[Ru('S_2')_2(PMe_3)_2]^{0/-}$ and $[Ru('S_2')_2(PMe_3)_2]^{-/2-}$ redox couples. The Ru complexes markedly differ from the homologous Fe compounds with respect to bonding, spectroscopic properties and reactivity, but stabilization of electron deficiency and high valency in these complexes is suggested to depend also on metal sulfur multiple bonding.

Introduction

Ascertainment of specific properties associated with metal sulfur centers — for example extended redox chemistry [2], stabilization of unusual metal oxidation states [3], as well as vacant coordination sites and electron deficiency [4, 5] — is important for understanding molecular processes occurring at the active sites of electron transferases and oxidoreductases that contain transition metals in sulfur dominated coordination spheres [6]. We recently reported syntheses, structures and properties of $[Fe('S_2')_2(PMe_3)_x]^n$ ($x=2$, $n=0$, -1; $x=1$, $n=0$; $'S_2'^{2-}$ = 1,2-benzenedithiolate(2–)) [5]. In contrast to dithiolene ligands of the type $S_2C_2R_2$ showing partial ligand oxidation in high valent complexes [2, 3a, 7], the $'S_2'^{2-}$ ligand in the Fe/'S₂' system exclusively acts as a dianionic dithiolate even when coordinated to Fe(IV) centers, and the electron deficiency of the high valent Fe centers is stabilized by sulfur iron π donation [5]. To analyze, whether this feature is primarily due to the 'S₂' ligand itself or also controlled by the metal, we investigated the homologous ruthenium complexes $[Ru('S_2')_2(PMe_3)_2]^n$ ($n=0$, -1). Preliminary results were reported elsewhere [8]. Inspite of numerous publications about dithiolenes surprisingly few ruthenium complexes are reported [9–14]. Our interest in related Ru('S₂') complexes dealt with reactivity and activation of small — preferably nitrogen containing — molecules [8, 15–17]. In this paper, spectroscopic and structural properties as well as redox behaviour and reactivity of

---

*For Part LXII see ref. 1.

**Author to whom correspondence should be addressed.

0020-1693/91/$3.50

$[Ru('S_2')_2(PMe_3)_2]^n$ ($n=0$, -1) are reported and compared to those of the homologous Fe complexes.

Experimental

General

Unless otherwise noted, all reactions and operations were carried out under nitrogen at room temperature by using standard Schlenk techniques. Solvents were dried and distilled before use. 1,2-Benzenedithiol, $'S_2'$-H_2 [18], PMe_3 [19] and $(NMe_4)[Fe('S_2')_2(PMe_3)_2]\cdot CH_3OH$ [5] were prepared as described in the literature. $RuCl_3\cdot xH_2O$ ($x\approx 3$) was obtained from Degussa; NaOMe from Aldrich; HBF_4 (54% in diethyl ether), NMe_4Cl and $FeCl_3$ from Merck; NBu_4OH (0.8 M methanolic solution) and NBu_4ClO_4 from Fluka. Spectra were recorded on the following instruments: NMR: Jeol FT-JNM-GX 270; IR (KBr discs): Perkin-Elmer 983; UV–Vis/near-IR: Shimadzu UV-3101 PC; mass spectra: Varian MAT 212. Magnetic moments were determined on a Johnson Matthey magnetic susceptibility balance at room temperature. Cyclic voltammetry was performed with a PAR 264 A potentiostat using a three electrode cell with glassy carbon ROTEL A working, Ag/AgCl reference and Pt counter electrodes. Potentials were referred to NHE via Cp_2Fe/Cp_2Fe^+ as internal standard.

Syntheses

$(NR_4)[Ru('S_2')_2(PMe_3)_2]$ (1) from $RuCl_3\cdot xH_2O$

(a) $(NMe_4)[Ru('S_2')_2(PMe_3)_2]\cdot CH_3OH$ (**1a**). A solution of $'S_2'$-H_2 (0.32 ml, 2.6 mmol) and NaOMe (285 mg, 5.3 mmol) in 10 ml of methanol was combined with a methanolic solution (10 ml) of $RuCl_3\cdot xH_2O$ (325 mg, 1.24 mmol). PMe_3 (0.5 ml, *c.* 5 mmol) was added and after 15 min of stirring the resulting air-sensitive violet reaction mixture was filtered. The filtrate was layered with methanol (10 ml) and subsequently with a solution of NMe_4Cl (165 mg, 1.5 mmol) in 10 ml of methanol. Black–red crystals of **1a** were separated after 3 days, washed with 15 ml of methanol and dried *in vacuo* for 1 day. Yield: 310 mg (39%). *Anal.* Calc. for $C_{23}H_{42}NOP_2RuS_4$ (639.87): C, 43.2; H, 6.6; N, 2.2. Found: C, 43.3; H, 6.9; N, 1.9%.

(b) $(NBu_4)[Ru('S_2')_2(PMe_3)_2]$ (**1b**). $'S_2'$-H_2 (0.75 ml, 6.1 mmol) in 15 ml of THF was deprotonated with NBu_4OH (15.8 ml of an 0.8 M solution in methanol, 12.6 mmol) and reacted with a solution of $RuCl_3\cdot xH_2O$ (770 mg, 2.95 mmol) in 15 ml of THF. PMe_3 (1.3 ml, *c.* 13 mmol) was added and after filtration the volume of the air-sensitive violet–red filtrate was reduced *in vacuo* to 15 ml. Upon addition of diethyl ether (80 ml) and cooling to −30 °C for 14 days dark red crystals of **1b** precipitated which were separated, washed with 30 ml of diethyl ether and 80 ml of H_2O and dried *in vacuo* for 1 day. Yield: 1.01 g (44%). *Anal.* Calc. for $C_{34}H_{62}NP_2RuS_4$ (776.15): C, 52.6; H, 8.1; N, 1.8. Found: C, 52.3; H, 8.4; N, 1.5%.

$[Ru('S_2')_2(PMe_3)_2]$ (2) from $RuCl_3\cdot xH_2O$

A stirred solution of $RuCl_3\cdot xH_2O$ (365 mg, 1.40 mmol) in 20 ml of methanol was treated with a solution of $'S_2'$-H_2 (0.35 ml, 2.9 mmol) and NaOMe (325 mg, 6.0 mmol) in 20 ml of methanol. PMe_3 (0.6 ml, *c.* 6 mmol) was added and after filtration air was bubbled through the violet filtrate for 10 min. Violet microcrystals of **2** precipitated. They were filtered off, washed with 40 ml of methanol and dried *in vacuo* for 1 day. The crude product (515 mg, 69%) was suspended in 50 ml of toluene and after addition of PMe_3 (0.5 ml, *c.* 5 mmol) the mixture was refluxed for 15 min and filtered while hot. Slow cooling of the filtrate to 20 °C yielded black crystals of **2**, which were separated after 2 days, washed with toluene and n-hexane and dried *in vacuo* for 8 h. Yield: 320 mg (43%, related to $RuCl_3\cdot xH_2O$). *Anal.* Calc. for $C_{18}H_{26}P_2RuS_4$ (533.68): C, 40.5; H, 4.9; S, 24.0. Found: C, 40.7; H, 5.0; S, 23.9%. Recrystallization from CH_2Cl_2 (+20 °C/−30 °C) supplied lower yields.

2 by Oxidation of 1b with H^+

1b (855 mg, 1.10 mmol) in 35 ml of methanol was introduced into a 50 ml Schlenk tube equipped with a septum inlet and connected to a gas burette. One equivalent of HCl in methanol (1.2 ml of a 0.92 M solution, 1.1 mmol) was injected in one portion to the stirred suspension. A pale violet solid immediately precipitated and the colour of the overlying solution changed from violet–red to pale brownish. No gas evolution was observed, even after 15 min of additional stirring. The precipitate was filtered off, washed with 40 ml of methanol and dried *in vacuo* for 1 h. Yield: 540 mg (92%) of **2** which was characterized by ^1H NMR and IR spectroscopy. Analogous results were obtained when HBF_4 in diethyl ether instead of HCl in methanol was used.

$(HPMe_3)_2[Fe('S_2')_2]_2$ (3)

(a) From $Na_2[Fe('S_2')_2]_2$ and $HPMe_3Cl$.

(1) $HPMe_3Cl$. Methanolic HCl (5.5 ml of a 0.92 M solution, 5 mmol) was added to a solution of PMe_3 (0.5 ml, *c.* 5 mmol) in 10 ml of methanol. Volatile components were removed under reduced pressure and the colourless solid was dried *in vacuo* for 3 h.

(2) $(HPMe_3)_2[Fe('S_2')_2]_2$. $Na_2[Fe('S_2')_2]_2$ was generated *in situ* by combining a solution of $'S_2'$-H_2 (0.52

ml, 4.2 mmol) and NaOMe (460 mg, 8.5 mmol) in 20 ml of methanol with a methanolic solution (20 ml) of $FeCl_3$ (340 mg, 2.10 mmol). After filtration, the black–red solution was layered with methanol (10 ml) and subsequently with $HPMe_3Cl$ (250 mg, 2.2 mmol) in 10 ml of methanol. After 4 days, black crystals of **3** were separated, washed with 50 ml of methanol and dried *in vacuo* for 6 h. Yield: 690 mg (79%). ^{1}H NMR (d_6-DMSO) δ 5.8 (1H, d, 500 Hz($^1J_{PH}$), P*H*), 1.45 (9H, s, P(C*H*$_3$)$_3$), −29.6 −34.2 (4H each, both s(broad), C_6H_4); ^{31}P NMR (d_6-DMSO) δ 15 (d, 500 Hz($^1J_{PH}$)). *Anal.* Calc. for $C_{30}Fe_2H_{36}P_2S_8$ (826.77): C, 43.6; H, 4.4. Found: C, 43.9; H, 4.5%.

(b) From $(NMe_4)[Fe(‘S_2’)_2(PMe_3)_2]\cdot CH_3OH$ and H^+. HCl in methanol (2.0 ml of a 0.92 M solution, 1.84 mmol) was added to a stirred dark violet–red methanolic solution (30 ml) of $(NMe_4)[Fe(‘S_2’)_2(PMe_3)_2\cdot CH_3OH$ (550 mg, 0.92 mmol). A violet–black microcrystalline precipitate immediately formed which was filtered off, washed with 30 ml of methanol and dried *in vacuo* for 1 day. IR, ^{1}H and ^{31}P NMR spectra of this compound were identical with those of **3** prepared according to method (a). Yield: 350 mg (92%). Analogous results were obtained when HBF_4 in diethyl ether (54%) instead of HCl in methanol was used.

X-ray structure determinations

Black crystals of $[Ru(‘S_2’)_2(PMe_3)_2]$ (**2**) were obtained from dichloromethane (+20 °C/−30 °C), and dark red columnar crystals of $(NMe_4)[Ru(‘S_2’)_2(PMe_3)_2]\cdot CH_3OH$ (**1a**) formed after storage of a methanolic $Na[Ru(‘S_2’)_2(PMe_3)_2]$ solution layered with NMe_4Cl in methanol for 3 days at 20 °C. The single crystals were sealed under N_2 in glass capillaries. The structures were solved by direct methods (SHELXTL PLUS). Non-hydrogen atoms were refined anisotropically, the aromatic hydrogen atoms were calculated for ideal geometry and restricted during refinement; the methyl hydrogen atoms were calculated for ideal tetrahedra and rotated around the central carbon atom during refinement; the isotropic H atoms were refined with common temperature factors. Refinement of the hydroxyl fragment of the methanol molecule in **1a** as rigid group produced unsatisfactory results for the position of the H atom; therefore, it was taken over from the difference Fourier map. The unit cell for **1a** contains two independent half molecules, each completed by the symmetry of the crystal. Table 1 summarizes crystallographic data, the fractional atomic coordinates are given in Table 2.

Results and discussion

Syntheses, characterization and spectra

$(NBu_4)[Ru(‘S_2’)_2(PMe_3)_2]\cdot THF$ was obtained previously and unexpectedly when $(NBu_4)[Ru(‘S_2’)_2(NO)]$ was reacted with an 160-fold excess of PMe_3 in boiling THF for 7 days; its oxidation by H^+, PhN_2BF_4 or O_2 yielded $[Ru(‘S_2’)_2(PMe_3)_2]$ (**2**) [8]. More conveniently and in analogy to the corresponding iron complexes [5], $(NR_4)[Ru(‘S_2’)_2(PMe_3)_2]$ (**1**) and $[Ru(‘S_2’)_2(PMe_3)_2]$ (**2**) are synthesized in one step reactions from $RuCl_3\cdot xH_2O$, $‘S_2’^{2-}$ and PMe_3 in the absence (**1**) or presence (**2**) of O_2 (eqn. (1)).

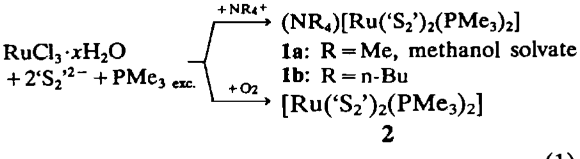

$$\mathrm{RuCl_3\cdot}x\mathrm{H_2O} + 2‘\mathrm{S_2}’^{2-} + \mathrm{PMe_{3\,exc.}} \begin{cases} \xrightarrow{+\mathrm{NR_4}^+} (\mathrm{NR_4})[\mathrm{Ru}(‘\mathrm{S_2}’)_2(\mathrm{PMe_3})_2] \\ \quad \mathbf{1a}\text{: R = Me, methanol solvate} \\ \quad \mathbf{1b}\text{: R = n-Bu} \\ \xrightarrow{+\mathrm{O_2}} [\mathrm{Ru}(‘\mathrm{S_2}’)_2(\mathrm{PMe_3})_2] \\ \quad \mathbf{2} \end{cases} \qquad (1)$$

The NR_4^+ salts are very soluble in polar solvents (**1a**, R = Me: DMSO, DMF; **1b**, R = Bu: DMSO, DMF, THF, acetone, CH_2Cl_2); neutral **2** is moderately soluble in CH_2Cl_2, $CHCl_3$, THF, toluene and CS_2.

1 is paramagnetic; in solid state (295 K), the magnetic moments of **1a** (1.33 μ_B) and **1b** (1.34 μ_B) are lower than the expected spin only value of low spin Ru(III), probably due to spin orbit coupling. Remarkably, **2** is diamagnetic. Although it compares in this respect with neutral dithiolene adducts of the type $[Ru(S_2C_2(CF_3)_2)_2(XPh_3)_2]$ (X = P, As, Sb) [11], pseudooctahedral Ru(IV) complexes usually possess magnetic moments of about 2.8 μ_B [20], and diamagnetism is generally found for five- and seven-coordinate Ru(IV) complexes [21]. In contrast, the magnetic moments of corresponding $[Fe(‘S_2’)_2(PMe_3)_2]^n$ are 2.00 μ_B ($n = -1$) and 2.75 μ_B ($n = 0$), consistent with low spin Fe(III) and Fe(IV) centers, respectively [5].

NMR data of **1a**, **1b** and **2** are summarized in Table 3. In the ^{1}H NMR spectra, the proton signals of the ‘S_2’ and PMe_3 ligands in **1a** and **1b** are shifted paramagnetically to high field. ^{31}P NMR data were obtained only for **2** (CD_2Cl_2, −24.5 ppm). For **1a** and **1b** no phosphorus signals could be observed; the ^{31}P NMR signal at +37 ppm previously reported for $(NBu_4)[Ru(‘S_2’)_2(PMe_3)_2]\cdot THF$ [8] could not be detected and was probably due to an impurity of $OPMe_3$. The $^{13}C\{^1H\}$ NMR spectrum of **2** displays three signals for the C_6 rings and one peak for the methyl groups; in comparison to other Ru(‘S_2’) complexes [16], the signal of the sulfur substituted carbon atoms (167.7 ppm) is shifted about 15 ppm to lower

TABLE 1. Crystallographic data for **1a** and **2**

Compound	$(NMe_4)[Ru(\text{'}S_2\text{'})_2(PMe_3)_2]\cdot CH_3OH$ (**1a**)	$[Ru(\text{'}S_2\text{'})_2(PMe_3)_2]$ (**2**)
Formula	$C_{23}H_{42}NOP_2RuS_4$	$C_{18}H_{26}P_2RuS_4$
Molecular weight	639.87	533.68
Crystal dimensions (mm)	0.50×0.25×0.25	0.40×0.30×0.20
Space group	$P\bar{1}$	$P2_1/c$
Cell dimensions		
a (pm)	882.6(3)	927.3(3)
b (pm)	935.1(2)	1012.0(3)
c (pm)	1800.1(4)	1220.2(5)
α (°)	92.27(1)	90.00(0)
β (°)	92.58(2)	102.35(3)
γ (°)	94.60(2)	90.00(0)
V (pm^3)	1478(1)×10^6	1118(1)×10^6
Z	2	2
D_{calc} (g/cm^3)	1.44	1.58
μ (cm^{-1})	9.1	11.5
Wavelength (pm)	71.073	71.073
Temperature of measurement (K)	200	293
R/R_w	0.045/0.039	0.031/0.027

field and indicates partial carbon sulfur multiple bonding [22].

In the mass spectra (FD), the fragments $[Ru(\text{'}S_2\text{'})_2(PMe_3)]^+$ at $m/e = 458$ (**1a**, **1b** and **2**), $[Ru(\text{'}S_2\text{'})_2(PMe_3)_2]^+$ at $m/e = 534$ (**1b** and **2**) $\{(NBu_4)[Ru(\text{'}S_2\text{'})_2(PMe_3)]\}^+$ at $m/e = 700$ (**1b**) were observed. The occurrence of monophosphine fragments demonstrates facile loss of one PMe_3 group.

IR spectra of **1a** (δ_{PCH}: 940 cm^{-1}; δ_{ar}: 745 cm^{-1}) and analogous $(NMe_4)[Fe(\text{'}S_2\text{'})_2(PMe_3)_2]\cdot CH_3OH$ [5] are almost identical. In contrast, those of $[Fe(\text{'}S_2\text{'})_2(PMe_3)_2]$ [5] and analogous **2** are significantly different. Both complexes show δ_{PCH} and δ_{ar} bands (**2**: 940 and 746 cm^{-1}, respectively), but the Ru complex **2** additionally exhibits a very strong absorption at 1054 cm^{-1}. This absorption can be assigned to a ν_{CS} whose frequency indicates considerable double bond character of the CS bond [2a].

For recording electronic spectra, scrupulously purified and absolutely oxygen free solvents were necessary to obtain reproducible results. Dissolution of **1b** and **2** in THF or CH_2Cl_2 (not freshly distilled) yielded blue solutions. Upon addition of PMe_3 the original colours of **1b** (violet–red) and **2** (brown–violet) immediately returned and the electronic spectra of these solutions were identical to those of **1b** and **2** in freshly purified solvents. The nature of the blue species remains as yet unknown. UV–Vis/near-IR spectra ($\lambda = 400$–2000 nm) of **1b** and **2** are shown in Fig. 1, data are listed in Table 3.

Most striking is the very intense near-IR absorption ($\epsilon = 21\,750$ l mol^{-1} cm^{-1}, $\lambda = 1192$ nm) of neutral **2**. Spectra in toluene, CH_2Cl_2 and THF proved to be absolutely identical even when an excess of HCl was added, excluding assignment of this absorption to sulfur $n \rightarrow \pi^*$ or ligand metal CT transitions.

Near-IR absorptions of much lower intensity were also observed for anionic $[Ru(\text{'}S_2\text{'})_2(PMe_3)_2]^-$. They proved to be practically identical for the NMe_4^+ salt **1a** in DMSO and the NBu_4^+ salt **1b** in DMSO and THF, ruling out any influence of cation or solvent on these low energy transitions.

In contrast, the homologous Fe complexes $[Fe(\text{'}S_2\text{'})_2(PMe_3)_2]^n$ ($n = 0, -1$) display only very weak absorptions in the near-IR region ($\epsilon < 1600$ l mol^{-1} cm^{-1}) [5]. Near-IR data of the related Ru complexes $[Ru(S_2C_2(CF_3)_2)_2(XPh_3)_n]$ (X = P, As, Sb; $n = 1, 2$) [11] are not reported.

Intense long wavelength ($\epsilon > 15\,000$ l mol^{-1} cm^{-1}, $\lambda > 700$ nm) electronic transitions are characteristic for high valent metal dithiolenes [7]. They are assigned to $\pi \rightarrow \pi^*$ transitions between molecular orbitals highly delocalized over metal, sulfur and unsaturated C–C bonds [7], and the strong near-IR band of **2** may indicate that a similar delocalization exists in $[Ru(\text{'}S_2\text{'})_2(PMe_3)_2]$ (**2**).

Because electronic, magnetic, IR and NMR properties indicated that bonding of Ru and analogous Fe complexes significantly differed, we carried out X-ray structure determinations of **1a** and **2** in order to check whether these differences could be substantiated by structural data.

X-ray structure determinations

The crystal lattice of **1a** contains discrete NMe_4^+ cations and $[Ru(\text{'}S_2\text{'})_2(PMe_3)_2]^-$ anions, that of **2**

TABLE 2. Fractional atomic coordinates ($\times 10^4$) and isotropic thermal parameters ($pm^2 \times 10^{-1}$) of the non-hydrogen atoms for **1a** and **2**

	x	y	z	U_{eq} [a]
(NMe$_4$)[Ru('S$_2$')$_2$(PMe$_3$)$_2$]·CH$_3$OH (**1a**)				
Ru(1)	5000	5000	5000	19(1)
P(1)	7041(1)	3539(1)	5221(1)	27(1)
C(1)	6506(6)	1651(5)	5352(3)	45(2)
C(2)	8431(6)	3476(6)	4514(3)	45(2)
C(3)	8258(6)	4004(6)	6063(3)	45(2)
S(1)	5626(1)	5347(1)	3754(1)	25(1)
S(2)	6719(1)	6998(1)	5310(1)	27(1)
C(15)	7415(5)	7585(4)	4469(2)	23(1)
C(14)	8454(5)	8793(4)	4469(3)	30(1)
C(13)	9005(5)	9297(5)	3809(3)	34(2)
C(12)	8542(5)	8576(5)	3138(3)	35(2)
C(11)	7541(5)	7376(5)	3127(2)	32(1)
C(10)	6940(5)	6858(4)	3787(2)	24(1)
Ru(2)	0	0	0	23(1)
P(2)	1471(1)	2106(1)	−330(1)	31(1)
C(4)	2123(7)	3413(6)	408(3)	58(2)
C(5)	519(6)	3220(6)	−983(3)	58(2)
C(6)	3209(6)	1805(6)	−793(3)	57(2)
S(3)	2159(1)	−1289(1)	81(1)	33(1)
S(4)	−167(1)	−684(1)	−1272(1)	33(1)
C(25)	1180(6)	−1943(5)	−1373(3)	34(2)
C(24)	1255(7)	−2701(5)	−2067(3)	48(2)
C(23)	2283(8)	−3709(6)	−2155(3)	60(2)
C(22)	3283(8)	−3974(6)	−1576(4)	61(2)
C(21)	3253(6)	−3223(5)	−888(3)	45(2)
C(20)	2192(5)	−2208(5)	−781(3)	32(1)
N(1)	3963(4)	903(4)	2605(2)	32(1)
C(31)	3488(6)	2387(5)	2555(3)	43(2)
C(32)	4353(7)	367(5)	1850(3)	49(2)
C(33)	5312(6)	908(6)	3135(3)	52(2)
C(34)	2699(6)	−40(5)	2889(3)	43(2)
O(1)	4203(5)	6894(5)	2349(2)	78(2)
C(35)	3036(7)	6197(7)	1884(3)	73(3)
[Ru('S$_2$')$_2$(PMe$_3$)$_2$] (**2**)				
Ru(1)	0	5000	5000	24(1)
S(1)	1816(1)	5387(1)	6606(1)	31(1)
S(2)	918(2)	6818(1)	4237(1)	34(1)
C(15)	2279(5)	7479(4)	5294(3)	29(2)
C(14)	2967(5)	8680(4)	5125(4)	37(2)
C(13)	4024(6)	9206(5)	5960(4)	43(2)
C(12)	4448(6)	8573(5)	6994(4)	43(2)
C(11)	3794(5)	7400(5)	7183(4)	37(2)
C(10)	2687(5)	6833(4)	6356(3)	28(1)
P(1)	1606(2)	3630(1)	4165(1)	39(1)
C(1)	1756(8)	4075(6)	2748(4)	67(3)
C(2)	1133(8)	1876(5)	4003(5)	71(3)
C(3)	3516(6)	3562(8)	4909(6)	97(3)

[a] Equivalent isotropic U defined as one third of the trace of the orthogonalized U_{ij} tensor.

discrete [Ru('S$_2$')$_2$(PMe$_3$)$_2$] molecules. No intermolecular contacts between Ru complex units could be found. Like the unit cell of the homologous (NMe$_4$)[Fe('S$_2$')$_2$(PMe$_3$)$_2$·CH$_3$OH [5], that of **1a** contains two different, independent halves of complex molecules, each completed by the symmetry of the crystal. Two methanol solvate molecules are connected via hydrogen bridges to *trans* sulfur atoms of one [Ru('S$_2$')$_2$(PMe$_3$)$_2$]$^-$ anion, while the other anion is unsolvated. Geometries and distances of both anions are approximately identical. Figure 2 shows the molecular structures of **2** and the solvated anion of **1a**. Crystallographic data of **1a** and **2** are summarized in Tables 1 and 2, selected distances and angles in Table 4.

The ruthenium atoms in **1a** and **2** are coordinated pseudooctahedrally by four sulfur atoms of two chelating 'S$_2$' ligands and by two *trans* PMe$_3$ phosphorus donors. **2** as well as both anions of **1a** possess crystallographically imposed centrosymmetry resulting in planar RuS$_4$ units and staggered arrangements of the phosphine methyl groups. In anionic **1a**, the Ru–S bonds cover the range from 233.7(2)–236.3(1) pm. The Ru–S distances in neutral **2** (232.7(1) and 230.7(1) pm) are only slightly but significantly shorter than in **1a** and distinctly shorter than in related pseudooctahedral [Ru(II)('S$_2$')(PMe$_3$)$_4$] (243.0 pm) [8]. Ru–S bond lengths in other Ru(III) and Ru(IV) sulfur ligand complexes range widely from 221 to 246 pm and depend also on coordination number and geometry [17, 21, 23].

In **1a** and **2**, interligand S···S (**1a**: av. 342.4 pm; **2**: 336.9 pm) are larger than intraligand S···S distances (**1a**: av. 321.4 pm; **2**: 318.2 pm), while in corresponding anionic [Fe('S$_2$')$_2$(PMe$_3$)$_2$]$^-$ the FeS$_4$ unit forms a nearly regular square with average S···S distances of 320 pm [5]. The upper limit of S···S intraligand distances is apparently determined by the 'bite' of the 'S$_2$' ligand, and because in [M('S$_2$')$_2$(PMe$_3$)$_2$]^n (M = Fe, Ru; $n = 0, -1$) Ru–S bonds are considerably longer than Fe–S bonds [5]; for M = Ru the MS$_4$ entity becomes rectangular.

Contrasting with Ru–S bond lengths, Ru–P distances in anionic **1a** are distinctly shorter (av. 237.8 pm) than in neutral **2** (241.7 pm). This indicates that the odd electron in **1** occupies a molecular orbital which must be bonding in character with respect to ruthenium and phosphorus.

The H atoms (H1d) forming the hydrogen bridges in [Ru('S$_2$')$_2$(PMe$_3$)$_2$]$^-$·2CH$_3$OH were located from a difference Fourier map. It yielded H1d–O1 distances of 102.7 pm, approximatively linear O1–H1d–S1 angles (171.9°) and H1d···S1 contacts of 219.9 pm that are shorter than H···S interactions in analogous [Fe('S$_2$')$_2$(PMe$_3$)$_2$]$^-$·2CH$_3$OH (243.7 pm) [5] and in X–H···S (X = N, O) hydrogen bridges of Fe$_4$S$_4$ type ferredoxines (~240 pm) [24]. Though obviously strong interactions, the O–H···S hydrogen bridges in [Ru('S$_2$')$_2$(PMe$_3$)$_2$]$^-$·2CH$_3$OH, precisely as in the analogous iron complex, do not influence

TABLE 3. NMR and UV–Vis/near-IR data of **1a**, **1b** and **2**

Complex	NMR[a] δ (ppm)		UV–Vis/near-IR[b] λ (nm) ($\epsilon \times 10^3$(l mol^{-1} cm^{-1}))
$(NMe_4)[Ru('S_2')_2(PMe_3)_2] \cdot CH_3OH$ (**1a**)	$^1H^c$	4.05 (1 H, m, CH_3OH) 3.15 (3 H, d, CH_3OH) 3.1 (12 H, s, $N(CH_3)_4$) −6.5 (18 H, s(broad), $P(CH_3)_3$) −9.5 (8 H, s(very broad), C_6H_4)	430 (2.610), 530 (sh, 1.500), 572 (2.840), 991 (4.840), 1098 (4.920)[g]
$(NBu_4)[Ru('S_2')_2(PMe_3)_2]$ (**1b**)	$^1H^c$	3.2−0.9 (36 H, m, $N(C_4H_9)_4$) −6.5 (18 H, s(broad), $P(CH_3)_3$) −9 (8 H, s(very broad), C_6H_4)	432 (2.210), 530 (sh, 1.400), 571 (2.530), 1004 (4.410), 1093 (4.600)[g]
			428 (2.330), 530 (sh, 1.400), 570 (2.500), 830 (sh, 1.300), 997 (4.010), 1092 (4.240)[h]
$[Ru('S_2')_2(PMe_3)_2]$ (**2**)	$^1H^{d,e}$	8.1 (4 H, m, C_6H_4) 6.8 (4 H, m, C_6H_4) 0.15 (18 H, s, $P(CH_3)_3$)	424 (3.430), 543 (2.140), 720 (sh, 0.500), 822 (1.410), 953 (1.700), 1192 (21.750), 1548 (1.060), 1654 (1.250)[i]
	$^1H^f$	7.9 (4 H, m, C_6H_4) 6.6 (4 H, m, C_6H_4) 0.05 (18 H, s, $P(CH_3)_3$)	
	$^{31}P\{^1H\}^{d,e}$	−24.5	
	$^{13}C\{^1H\}^d$	167.7, 130.5, 121.9 (C_6H_4) 10.1 ($P(CH_3)_3$)	

[a] s: singlet, d: doublet, m: multiplet. [b] 10^{-3} M solutions, sh: shoulder. [c] In d_6-DMSO. [d] In CD_2Cl_2. [e] cf. ref. 8. [f] In CS_2/C_6D_6 (9:1). [g] In DMSO. [h] In THF, excess PMe_3 added. [i] In THF.

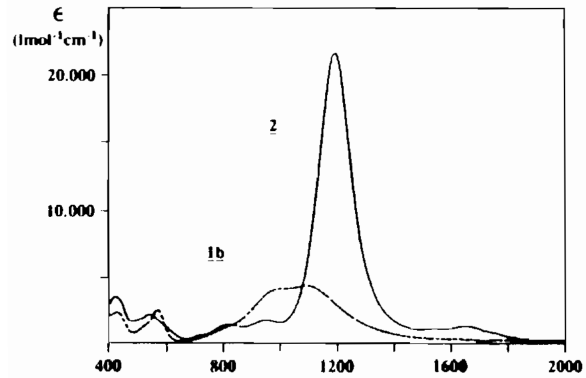

Fig. 1. UV–Vis/near-IR spectra of **1b** in the presence of PMe_3 and of **2**; THF, 1×10^{-3} M solutions.

the metal sulfur bond lengths very much and Ru1–S1 (236.3(1) pm) is only slightly longer than the other Ru–S distances in the solvated and unsolvated anions (av. 234.3 pm). In solution, the hydrogen bridges are apparently not maintained as indicated by the sharp methanol signals in the ^1H NMR spectrum of **1a**.

Discussion of bonding in 1 and 2

In the systems described here the question arises, whether the properties of the metal sulfur center are determined by bonding in the metal sulfur core only or also by the atoms beyond the sulfur donors, in particular, if unsaturated C–C bonds as in dithiolene ligands of the type $[S_2C_2R_2]^{n-}$ ($n=0$, 2) are involved. Structural data and spectroscopic results indicate that $[S_2C_2R_2]^{n-}$ ligands bind to metal centers in a form somewhere between dianionic dithiolates and (oxidized) neutral dithiodiketones [2, 3a, 7] and that assignment of oxidation states to the metal centers is not very meaningful. In contrast, oxidation of 1,2-benzenedithiolate to cyclohexadienedithiodiketone would require breaking up the aromatic system as illustrated by the limiting mesomeric structures I and II of a planar neutral $[M('S_2')_2]$ complex, and thus it should be much less favourable.

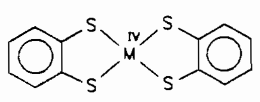

I

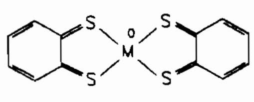

II

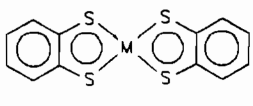

III

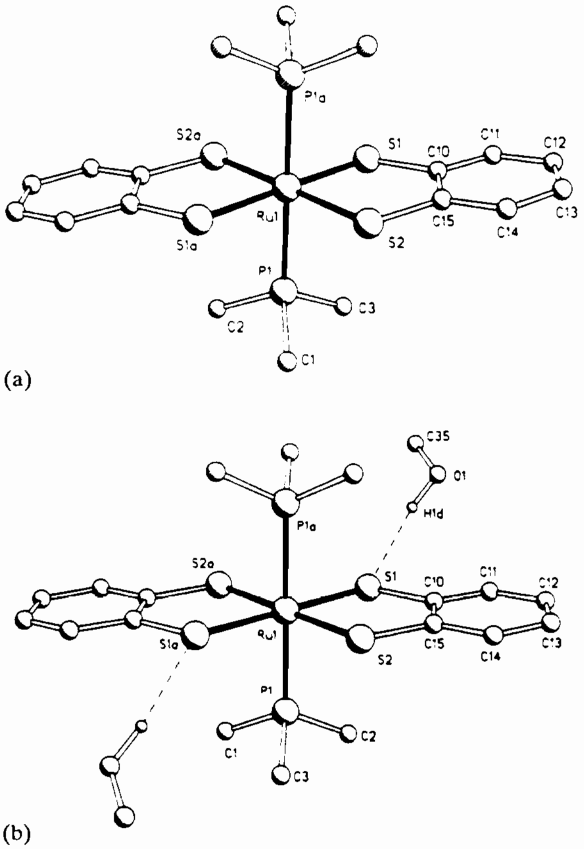

Fig. 2. Molecular structures of (a) $[Ru('S_2')_2(PMe_3)_2]$ (**2**) and (b) the solvated $[Ru('S_2')_2(PMe_3)_2]^- \cdot 2CH_3OH$ anion of **1a**. H atoms are omitted with the exception of H1d in (b).

In fact, bonding in the $[M('S_2')_2]$ core of $[Fe('S_2')_2(PMe_3)_2]$ [5] is best described by the limiting structure **I**. As indicated by the results outlined above, bonding in the analogous Ru complexes appears to be different, and in order to gain closer insight, we compared the C–S and C–C distances of **1a**, **2** and dibenzo-18-crown-S6, bzo$_2$-18S6 [25], that can be expected to contain a practically undisturbed 'S$_2$' entity (Table 5).

The average C–S bond lengths increase from neutral **2** via anionic **1a** to bzo$_2$-18S6. Comparable short average C–S bond distances as in **2** are reported for $[Mo('S_2')_3]$ (172.7(6) pm) and discussed to have considerable C=S double bond character [26]. Thus, the C–S distances in **2** could be indicative of C=S double bonds in **2**, the same would hold for **1a**, and the respective C–S distances in bzo$_2$-18S6 (177.2(5) pm) then could be regarded as pure C_{ar}–S single bonds; practically identical C_{ar}–S distances (av. 177.6 pm) were found in $(C_6H_5S)_4C$ [27]. In conclusion, C–S bond lengths in **2** would point at a major contribution of the limiting mesomeric structure **II** to the overall bonding situation in **2**. Then, the C–C bonds within the benzene rings of **2** should exhibit alternating distances that differ from the bond lengths in bzo$_2$-18S6. This, however, is not the case. Though the C–C distances in the benzene rings of **2**, **1a**, and bzo$_2$-18S6 cover the range from 137–143 pm and appear to alternate within the standard deviations, corresponding C–C bonds of all three compounds are identical.

In conclusion, the structural data do not allow the apparent alternation of C–C distances in the benzene rings to be traced back to a cyclohexadienedithiodiketone character of the $C_6H_4S_2$ units caused by oxidation of 1,2-benzenedithiolate. The comparison of **2** and **1a** with bzo$_2$-18S6 rather suggests that it is simply due to the distortion of the benzene rings introduced by the *ortho*-disubstitution.

In order to explain the C–S distances of **2** which are distinctly shorter than in bzo$_2$-18S6 and indicate double bond character, it is then necessary to assume a delocalized π-electron system as illustrated by the limiting mesomeric structure **III**. It extends beyond the sulfur donors but does not lead to a serious cyclohexadiene-like distortion of the C_6 rings. This description was previously applied to systems of the type $[M(S_2C_2R_2)_2]$ [7], and it can also explain the relatively short Ru–S distances, the very intense $\pi \rightarrow \pi^*$ near-IR transition, as well as NMR and IR properties of **2**. Of further interest is the shortening of the Ru–P and the lengthening of Ru–S and C–S bonds when neutral **2** is reduced by one electron to give anionic **1**. The changes indicate that the odd electron resides in an orbital that is not localized but extends over the $RuS_4C_4P_2$ unit and is bonding with respect to Ru–P and antibonding with respect to Ru–S and C–S. Thus, the Ru complexes **2** and **1** differ markedly in bonding from the analogous $[Fe('S_2')_2(PMe_3)_2]^n$ ($n=0, -1$) complexes [5] which do not exhibit π-electron delocalization beyond the sulfur donors nor into the metal phosphorus bonds.

Reactivity studies of $[M('S_2')_2(PMe_3)_2]^-$ (M=Ru, Fe) and electrochemistry of $[Ru('S_2')_2(PMe_3)_2]^n$ ($n=0, -1$)

$[Ru('S_2')_2(PMe_3)_2]$ (**2**) was originally obtained when $(NBu_4)[Ru('S_2')_2(PMe_3)_2]$ (**1b**) was reacted with one equivalent of HBF_4 and the resulting product was recrystallized from CH_2Cl_2; the oxidizing agent was suggested to be H^+ [8]. H_2 as reduction product of H^+, however, was not detected and thus it could not be excluded that the primary product was a hydride complex that reacted with CH_2Cl_2 to give **2** [28]. In order to settle this question we reexamined the reaction according to eqn. (2).

TABLE 4. Selected interatomic distances (pm) and angles (°) for **1a** and **2**[a]

$(NMe_4)[Ru('S_2')_2(PMe_3)_2]\cdot CH_3OH$ (**1a**)			
$[Ru('S_2')_2(PMe_3)_2]^-\cdot 2CH_3OH$			
Ru(1)–P(1)	237.5(2)	Ru(1)–S(1)	236.3(1)
Ru(1)–S(2)	234.3(1)	S(1)–C(10)	175.2(4)
S(2)–C(15)	175.1(4)	C(15)–C(14)	139.7(6)
C(15)–C(10)	141.0(5)	C(14)–C(13)	139.0(6)
C(13)–C(12)	138.8(6)	C(12)–C(11)	137.0(6)
C(11)–C(10)	141.1(6)	O(1)–C(35)	140.0(7)
O(1)–H(1D)	102.7	H(1D)···S(1)	219.9
S(1)···S(2)	321.5	S(1)···S(2A)	343.6
P(1)–Ru(1)–S(1)	92.9(1)	P(1)–Ru(1)–S(2)	87.6(1)
S(1)–Ru(1)–S(2)	86.2(1)	S(1)–Ru(1)–P(1A)	87.1(1)
S(2)–Ru(1)–P(1A)	92.4(1)	S(1)–Ru(1)–S(2A)	93.8(1)
O(1)–H(1D)···S(1)	171.9		
$[Ru('S_2')_2(PMe_3)_2]^-$			
Ru(2)–P(2)	238.1(1)	Ru(2)–S(3)	233.7(2)
Ru(2)–S(4)	234.8(1)	S(3)–C(20)	174.7(5)
S(4)–C(25)	174.9(5)	C(25)–C(24)	141.9(7)
C(25)–C(20)	140.2(6)	C(24)–C(23)	136.9(9)
C(23)–C(22)	137.9(9)	C(22)–C(21)	140.1(8)
C(21)–C(20)	140.0(7)		
S(3)···S(4)	321.2	S(3)···S(4A)	341.1
P(2)–Ru(2)–S(3)	91.6(1)	P(2)–Ru(2)–S(4)	87.0(1)
S(3)–Ru(2)–S(4)	86.6(1)	S(3)–Ru(2)–P(2A)	88.4(1)
S(4)–Ru(2)–P(2A)	93.0(1)	S(3)–Ru(2)–S(4A)	93.4(1)
$[Ru('S_2')_2(PMe_3)_2]$ (**2**)			
Ru(1)–S(1)	232.7(1)	Ru(1)–S(2)	230.7(1)
Ru(1)–P(1)	241.7(1)	S(1)–C(10)	173.0(4)
S(2)–C(15)	173.4(4)	C(15)–C(14)	140.9(6)
C(15)–C(10)	142.9(5)	C(14)–C(13)	136.2(6)
C(13)–C(12)	139.5(6)	C(12)–C(11)	137.4(6)
C(11)–C(10)	140.0(5)		
S(1)···S(2)	318.2	S(1)···S(2A)	336.9
S(2)–Ru(1)–S(1)	86.7(1)	P(1)–Ru(1)–S(1)	93.0(1)
P(1)–Ru(1)–S(2)	88.4(1)		

[a] e.s.d.s. are given in parentheses.

$$\mathbf{1b} + 1HX \xrightarrow{MeOH/10\ s} \mathbf{2} + NBu_4X + \text{other products} \qquad (2)$$

$X^- = BF_4^-, Cl^-$

Upon addition of HBF_4 to **1b** in methanol, a violet solid immediately precipitated in approximately quantitative yield but again no gas evolution could be detected. The ^1H NMR spectra (CS_2/10% C_6D_6) of the precipitate and of **2** synthesized according to eqn. (1) (cf. Table 3) proved to be identical, in particular, they showed no M–H resonance signals. Analogous results were obtained by using HCl in methanol instead of HBF_4 in diethyl ether, thus any influence of the acid anions could be excluded.

These findings suggest that H^+ indeed is the oxidizing agent and **2** the direct oxidation product. The species resulting from proton reduction, however, remains unknown; possibly, originating $H^\bullet$ radicals react with solvent molecules or NBu_4^+ cations.

The reaction of the homologous iron complex $[Fe('S_2')_2(PMe_3)_2]^-$ with H^+ (eqn. (3)), which was carried out for the purpose of comparison, took a completely different course.

$$(NMe_4)[Fe('S_2')_2(PMe_3)_2]\cdot CH_3OH$$
$$+ 2HX \xrightarrow[-NMe_4X/-HPMe_3X]{MeOH} \underset{\mathbf{3}}{\tfrac{1}{2}(HPMe_3)_2[Fe('S_2')_2]_2} \qquad (3)$$

$X^- = Cl^-, BF_4^-$

Here, two equivalents of H^+ were required to achieve complete conversion. No oxidation but decoordination and protonation of both phosphine ligands took place causing formation of binuclear [29] $[Fe(III)('S_2')_2]_2^{2-}$, which was isolated as the $HPMe_3^+$ salt **3**. **3** was also obtained by direct synthesis (eqn. (4)) and characterized by ^1H and ^{31}P NMR spectra.

TABLE 5. Average C–S and C–C distances in **1a**, **2** and bzo$_2$-18S6

Distances (pm)[a]	$[Ru('S_2')_2(PMe_3)_2]$ (**2**)	$(NMe_4)[Ru('S_2')_2(PMe_3)_2]\cdot CH_3OH$ (**1a**)	bzo$_2$-18S6[b]
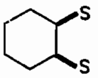	173.2(4)	175.2(4)[c] 174.8(5)[d]	177.2(5)
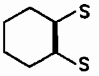	142.9(5)	141.0(5)[c] 140.2(6)[d]	138.9(8)
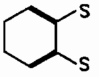	140.5(6)	140.4(6)[c] 141.0(7)[d]	139.1(7)
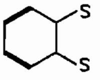	136.8(6)	138.0(6)[c] 138.5(9)[d]	137.3(8)
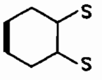	139.5(6)	138.8(6)[c] 137.9(9)[d]	139.4(9)

[a] C–C and C–S bonds regarded are marked with thick lines. [b] Ref. 25. [c] For $[Ru('S_2')_2(PMe_3)_2]^- \cdot 2CH_3OH$. [d] For $[Ru('S_2')_2(PMe_3)_2]^-$.

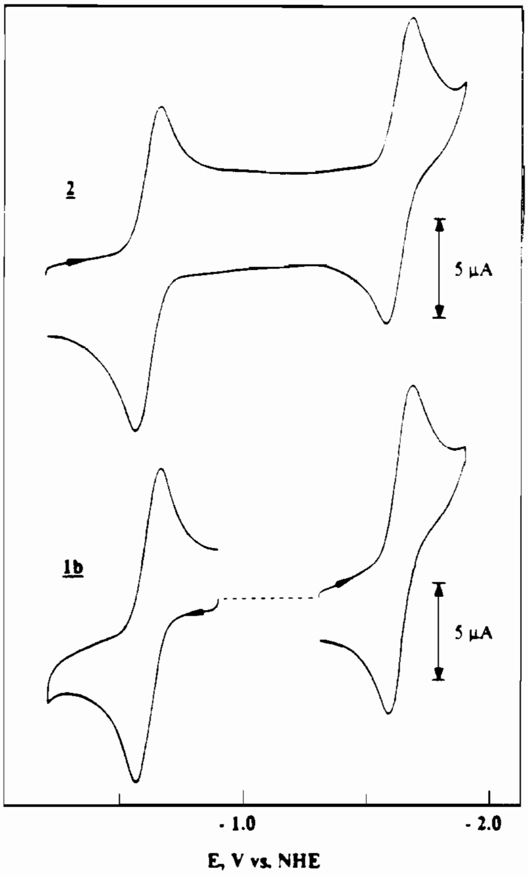

Fig. 3. Cyclic voltammograms of **2** and **1b** in the presence of PMe$_3$; THF, 1×10^{-4} M solutions, 0.10 M NBu$_4$ClO$_4$. Scan rate = 0.100 V s^{-1}.

$$FeCl_3 + 2Na_2'S_2' \xrightarrow[-3\,NaCl]{MeOH} Na[Fe('S_2')_2] \xrightarrow[-NaCl]{+HPMe_3Cl} \mathbf{13} \tag{4}$$

The different behaviour of $[Fe('S_2')_2(PMe_3)_2]^-$ versus $[Ru('S_2')_2(PMe_3)_2]^-$ towards protons can be traced back, at least partially, to redox potentials. In contrast to the $[Fe('S_2')_2(PMe_3)_2]^{0/-}$ couple (−0.30 V versus NHE) [5], the $[Ru('S_2')_2(PMe_3)_2]^{0/-}$ couple exhibits a considerably more negative potential as shown by the cyclic voltammograms (CVs) of **1b** and **2** in THF, recorded in the range from −0.2 to −1.9 V versus NHE (Fig. 3). In the presence of PMe$_3$, they display two quasi-reversible redox waves at −0.59 and −1.60 V assigned to $[Ru('S_2')_2(PMe_3)_2]^{0/-}$ and $[Ru('S_2')_2(PMe_3)_2]^{-/2-}$ couples, respectively. As in the case of recording the electronic spectra, meticulously purified solvents were necessary in order to obtain the CVs, and here, in order to observe quasi-reversibility of the redox processes, a drop of extra PMe$_3$ has to be added. Without phosphine, the second reduction of **2** became irreversible, and for **1b** no redox waves could be observed at all. With extra PMe$_3$ present, the CV of **1b** showed identical redox waves as **2**. Selected electrochemical parameters are listed in Table 6.

Because PMe$_3$ had to be added, the anodic electrochemistry of **1b** could not be investigated. In the anodic range and without PMe$_3$ **2** displayed two irreversible oxidation peaks at +0.54 and +0.73 V and two small irreversible reduction peaks at +0.35 and +0.67 V.

TABLE 6. Selected electrochemical parameters

Complex	E_{pc} (V)[a, d]	E_{pa} (V)[b, d]	ΔE_p (V)[c, d]	E (V)[e]	I_{pa}/I_{pc}[f]	
[Ru('S_2')$_2$(PMe_3)$_2$] **(2)**	−0.634	−0.537	0.097	−0.59	1.0	first reduction
	−1.650	−1.550	0.100	−1.60	0.9	second reduction
(NBu_4)[Ru('S_2')$_2$(PMe_3)$_2$] **(1b)**	−0.634	−0.534	0.100	−0.58	0.9[g]	oxidation
	−1.651	−1.534	0.117	−1.59	0.9	reduction

[a] CV, reduction peak. [b] CV, oxidation peak. [c] E_{pa}–E_{pc}. [d] Function of scan rate (0.020, 0.050, 0.100 V/s): values listed were obtained at scan rate = 0.100 V/s. [e] (Formal) redox potential. [f] Peak current ratio. [g] I_{pc}/I_{pa} (V) vs. NHE, THF, 1×10^{-4} M solutions, PMe_3 excess added, 0.10 M NBu_4ClO_4, room temperature.

TABLE 7. Summary of similarities and differences in iron and ruthenium [M('S_2')$_2$(PMe_3)$_2$]^n ($n=0$, -1)[a] complexes

Complex[a]	$[Fe]^0$ [b]	$[Fe]^{-1}$ [b]	$[Ru]^0$	$[Ru]^{-1}$
Structure	pseudooctahedral, *trans*-PMe_3		pseudooctahedral, *trans*-PMe_3	
*d*M–S(av.)	shorter	longer	shorter	longer
*d*C–S(av.)	equal	equal	shorter	longer
*d*M–P(av.)	equal	equal	longer	shorter
Magnetism (unpaired e^-)	para (2)	para (1)	dia	para (1)
Near-IR electronic transitions(s)	weak	very weak	very strong	medium
IR spectra	insignificant	insignificant	very strong ν_{CS}	insignificant
Redox potentials $[M]^{0/-}/[M]^{-/2-}$	−0.3/−1.0		−0.6/−1.6	
Oxidation state	Fe(IV)[c]	Fe(III)[c]	–[d]	–[d]
π Bonding	localized within the FeS_4 core		delocalized over $RuS_4C_4P_2$ unit	

[a] Abbreviated: $[M]^n$. [b] Ref. 5. [c] Mössbauer spectroscopy. [d] Not determined.

The $[Ru('S_2')_2(PMe_3)_2]^{0/-}$ (−0.6 V) and $[Ru('S_2')_2(PMe_3)_2]^{-/2-}$ (−1.6 V) redox couples are both distinctly more negative than the corresponding Fe(IV/III) and Fe(III/II) couples of the homologous iron complexes (−0.3 and −1.0 V, respectively) [5], that is, even $[Ru('S_2')_2(PMe_3)_2]^-$ containing Ru(III), the most common ruthenium oxidation state, becomes strongly reducing; accordingly, neutral [Ru('S_2')$_2$(PMe_3)$_2$] is more stable towards electrochemical reduction than analogous [Fe('S_2')$_2$(PMe_3)$_2$]. A similar behaviour was observed for the dithiolene complex couples $[M(S_2C_2(CF_3)_2)_2(XPh_3)]^{0/-}$ (M = Fe, Ru; X = P, As, Sb) [11, 30] and confirms the general trend that higher oxidation states become more stable with the heavier elements of a group. The redox potentials of $(Ru(S_2C_2(CF_3)_2)_2(XPh_3)]^{0/-}$ (X = P, As, Sb) [11], however, lie in the range around +0.4 V and are about 1.0 V more positive than those of the $[Ru('S_2')_2(PMe_3)_2]^{0/-}$ couple, showing again the distinct difference between $S_2C_2R_2$ and aromatic 'S_2' ligands.

The extremely negative potentials (−1.6 V) of the $[Ru('S_2')_2(PMe_3)_2]^{-/2-}$ couple may be the reason why salts of the dianion have not yet been isolated.

Discussion

The similarities and differences of Ru and Fe $[M('S_2')_2(PMe_3)_2]^n$ ($n=0$, -1) complexes are summarized in Table 7 and will be discussed in conclusion.

Similar, of course, are the composition and the gross structures with respect to the pseudooctahedral metal coordination by four sulfur donors in a plane and two *trans* PMe_3 ligands. Similar also are the decrease in M–S bond lengths going from anionic to neutral complexes, which, however, would be anticipated as a generally observed feature, and the existence of neutral, mono- and dianionic species. But here already the similarities end, because in every other respect the Fe and Ru systems are different.

The distinctions indicate a different bonding situation. In the Fe complexes, M–S π bonding is confined to the FeS_4 core and high valent Fe centers are stabilized by dianionic 'S_2'$^{2-}$ ligands [5]; the Ru complexes, however, display extended π-electron delocalization over $RuS_4C_4P_2$ entities. With regard to the different bonding, the different reactivity of

Fe and Ru complexes is no longer surprising. It is noted, that also in comparison to complexes with $S_2C_2R_2$ type ligands distinctions are observed. This is shown, for example, by the redox potentials of $[Ru(S_2C_2(CF_3)_2)_2(PPh_3)]^{0/-}$ (+0.5 V) [11] and $[Ru('S_2')_2(PMe_3)_2]^{0/-}$ (−0.6 V) that differ by more than 1 V.

Review articles [2, 3a, 7, 31] tend to generalize properties of dithiolenes, under which term complexes with non-aromatic 1,2-$S_2C_2R_2$ as well as aromatic 1,2-$S_2C_6R_4$ type ligands are comprised. This may be helpful for the purpose of classification, but implies a generality which does not really exist. $[Fe('S_2')_2(PMe_3)_2]^n$ and $[Ru('S_2')_2(PMe_3)_2]^n$ ($n = 0, -1$) seem to differ only in the metal center, but in fact, as was shown above, they also differ in many other respects. This illustrates that a general principle of bonding and reactivity cannot be anticipated even for *the very same* ligand coordinated to *homologous* metals with *identical* coligands — and this may hold even more for 1,2-$S_2C_2R_2$ versus 1,2-$S_2C_6R_4$ complexes.

Supplementary material

Further details of X-ray crystal structure analyses have been deposited and can be obtained from the Fachinformationszentrum Karlsruhe, D-7514 Eggenstein-Leopoldshafen 2 by citing the deposition nos. CSD 320187 ($(NMe_4)[Ru('S_2')_2(PMe_3)_2]\cdot CH_3OH$ (**1a**)), CSD 320186 ($[Ru('S_2')_2(PMe_3)_2]$ (**2**)), the authors and the reference.

Acknowledgements

These investigations were supported by the Deutsche Forschungsgemeinschaft, by the Fonds der Chemischen Industrie, and by a donation of $RuCl_3\cdot xH_2O$ by Degussa AG, Hanau, F.R.G. We gratefully acknowledge this support.

References

1 D. Sellmann, M. Geck and M. Moll, *J. Am. Chem. Soc.,* in press.

2 (a) J. A. McCleverty, *Prog. Inorg. Chem., 10* (1968) 49; (b) E. Hoyer, W. Dietzsch and W. Schroth, *Z. Chem., 11* (1971) 41.

3 (a) R. P. Burns and C. A. McAuliffe, *Adv. Inorg. Chem. Radiochem., 22* (1979) 303, and refs. therein; (b) R. P. Burns, F. P. McCullough and C. A. McAuliffe, *Adv. Inorg. Chem. Radiochem., 23* (1980) 211, and refs. therein.

4 D. Sellmann, W. Ludwig, G. Huttner and L. Zsolnai, *J. Organomet. Chem., 294* (1985) 199.

5 D. Sellmann, M. Geck, F. Knoch, G. Ritter and J. Dengler, *J. Am. Chem. Soc., 113* (1991) 3819.

6 (a) T. G. Spiro (ed.), *Iron Sulfur Proteins, Metal Ions in Biology,* Vol. 4, Wiley, New York, 1982; (b) T. G. Spiro (ed.), *Molybdenum Enzymes, Metal Ions in Biology,* Vol. 7, Wiley, New York, 1985; (c) T. R. Hawkes, P. A. McLean and B. E. Smith, *Biochem. J., 217* (1984) 217.

7 U. T. Mueller-Westerhoff and B. Vance, in G. Wilkinson and R. D. Gillard (eds.), *Comprehensive Coordination Chemistry,* Vol. 2, Pergamon, Oxford, 1987, Ch. 16.5, p. 595.

8 D. Sellmann, G. Binker and F. Knoch, *Z. Naturforsch., Teil B, 42* (1987) 1298.

9 (a) G. N. Schrauzer, H. W. Finck and V. Mayweg, *Angew. Chem., 76* (1964) 715; (b) G. N. Schrauzer, V. Mayweg, H. W. Finck, U. Müller-Westerhoff and W. Heinrich, *Angew. Chem., 76* (1964) 345.

10 R. E. DeSimone, *J. Am. Chem. Soc., 95* (1973) 6238.

11 J. Miller and A. L. Balch, *Inorg. Chem., 10* (1971) 1410.

12 J. D. Gilbert, D. Rose and G. Wilkinson, *J. Chem. Soc. A,* (1970) 2765.

13 (a) I. Bernal, A. Clearfield and J. S. Ricci, *J. Cryst. Mol. Struct., 4* (1974) 43; (b) A. Clearfield, E. F. Epstein and I. Bernal, *J. Coord. Chem., 6* (1977) 227.

14 T. B. Rauchfuss, D. P. S. Rodgers and S. R. Wilson, *J. Am. Chem. Soc., 108* (1986) 3114.

15 D. Sellmann and E. Böhlen, *Z. Naturforsch., Teil B, 37* (1982) 1026.

16 D. Sellmann and G. Binker, *Z. Naturforsch., Teil B, 42* (1987) 341.

17 D. Sellmann, I. Barth, F. Knoch and M. Moll, *Inorg. Chem., 29* (1990) 1822.

18 J. Degani and R. Fochi, *Synthesis, 7* (1976) 471.

19 W. Wolfsberger and H. Schmidbaur, *Synth. React. Inorg. Met.-Org. Chem., 4* (1974) 149.

20 (a) N. N. Greenwood and A. Earnshaw, *Chemistry of the Elements,* Pergamon, Oxford, 1984, p. 1262; (b) A. Y. Girgis, Y. S. Sohn and A. L. Balch, *Inorg. Chem., 14* (1975) 2327; (c) D. Pawson and W. P. Griffith, *J. Chem. Soc., Dalton Trans.,* (1975) 417.

21 (a) K. W. Given, B. M. Mattson and L. H. Pignolet, *Inorg. Chem., 15* (1976) 3152; (b) B. M. Mattson and L. H. Pignolet, *Inorg. Chem., 16* (1977) 488; (c) S. A. Koch and M. M. Millar, *J. Am. Chem. Soc., 105* (1983) 3362; (d) M. M. Millar, T. O'Sullivan, N. deVries and S. A. Koch, *J. Am. Chem. Soc., 107* (1985) 3714.

22 H.-O. Kalinowski, S. Berger and S. Braun, *^{13}C-NMR-Spektroskopie,* Thieme, Stuttgart, 1984, p. 77.

23 L. H. Pignolet, *Inorg. Chem., 13* (1974) 2051.

24 E. Adman, K. D. Watenpaugh and L. H. Jensen, *Proc. Natl. Acad. Sci. U.S.A., 72* (1975) 4854.

25 D. Sellmann and P. Frank, *Angew. Chem., 98* (1986) 1115; *Angew. Chem., Int. Ed. Engl., 25* (1986) 1107; (b) D. Sellmann, P. Frank and F. Knoch, *J. Organomet. Chem., 339* (1988) 345.

26 M. Cowie and M. J. Bennett, *Inorg. Chem., 15* (1976) 1584.

27 K. Kato, *Acta Crystallogr., Sect. B, 28* (1972) 606.

28 (a) H. D. Kaesz and R. B. Saillant, *Chem. Rev., 72* (1972) 231; (b) W. Kruse and R. H. Atalla, *J. Chem. Soc., Chem. Commun.,* (1968) 921; (c) A. Bainbridge, P. J. Craig and M. Green, *J. Chem. Soc. A,* (1968) 2715; (d) D. Sellmann and L. Zapf, *Z. Naturforsch., Teil B, 40* (1985) 380; (e) D. Sellmann, A. Fetz, M. Moll and F. Knoch, *Polyhedron, 8* (1989) 613.

29 (a) B. S. Kang, L. H. Weng, D. X. Wu, F. Wang, Z. Guo, L. R. Huang, Z. Y. Huang and H. Q. Liu, *Inorg. Chem., 27* (1988) 1128; (b) R. Weiss, *Dissertation,* Universität Erlangen-Nürnberg, 1990.

30 A. L. Balch, *Inorg. Chem., 6* (1967) 2158.

31 R. Eisenberg, *Prog. Inorg. Chem., 12* (1970) 295.